Giant ferromagnetic π-d interaction in a phthalocyanine molecule

H. Murakawa,[1] A. Kanda,[1] M. Ikeda,[1] M. Matsuda,[2] and N. Hanasaki[1]
[1]*Department of Physics, Graduate School of Science, Osaka University, Osaka 560-0043, Japan*
[2]*Graduate School of Science and Technology, Kumamoto University, Kumamoto 860-8555, Japan*
(Received 26 January 2015; revised manuscript received 27 July 2015; published 21 August 2015)

We experimentally demonstrate that the ferromagnetic intramolecular π-d interaction works between an itinerant π-electron spin and a localized d-electron's magnetic moment in the iron-phthalocyanine (Pc) molecular compound. The evaluation of the hidden π-d coupling is achieved by preparing the isolated $Fe(Pc)(CN)_2$ molecular solution with unpaired π- and d-electron spins, which is generated through the oxidization by iodine bromide (IBr). The monotonic increase of the magnetization with IBr addition and the saturation value of the Curie constant indicate the ferromagnetic π-d coupling. Furthermore, through the magnetization measurements of the single crystals of neutral π radical $Fe(Pc)(CN)_2 \cdot 2CHCl_3$, we reveal that the on-site π-d interaction in $Fe(Pc)(CN)_2$ is extremely large ($J_{\pi d}/k_B > 500$ K) among those in other molecular materials.

DOI: 10.1103/PhysRevB.92.054429 PACS number(s): 75.50.Xx, 33.15.Kr

I. INTRODUCTION

The interaction between delocalized and localized magnetic moments in a molecule is a fundamental source of various fascinating phenomena. In some molecular compounds including a transition metal ion, the interaction between an itinerant π- and localized d-electron spins, namely, π-d interaction ($J_{\pi d}$) is the key factor for the metal-insulator transition [1–5] and the magnetic-field-induced superconductivity [6,7]. The magnitude of $J_{\pi d}$ in the above typical π-d systems with spacially separate π-d sources is limited to be on the order of $\sim$10 K [8]. For the further development of molecular functionalities, the on-site intramolecular magnetic interaction between π and d or f electrons has a great advantage. In this regard, metal phthalocyanine (M-Pc), in which various kinds of lanthanide Ln as well as transition metal ion can be embedded at the center of the Pc ring [Fig. 1(a)] is an ideal system. Since the discovery of the functionalities as a single-molecule magnet in the lanthanide double-decker phthalocyanine Pc_2Ln (Ln = Tb, Dy, Ho, Er, Tm, and Yb) [9,10], the family of the magnetic phthalocyanine has been intensively investigated toward the application in the area of spintronics [11–13]. On the other hand, the transition-metal phthalocyanine [14] is prospective candidate to possess large on-site π-d interaction, which can significantly affect the charge carrier motion, providing an opportunity to control molecular conductivity by magnetic stimulus.

In fact, π-d interaction plays a crucial role in the remarkable giant negative magnetoresistance of $TPP[Fe(Pc)(CN)_2]_2$ [Fig. 1(b)], where TPP denotes tetraphenylphosphonium, just a closed shell cation [15–18]. According to the quantum chemical calculation, it has a quasi-one-dimensional conduction band with 3/4 filling, or 1/4 filling in terms of holes, along the stacking direction of the Pc plane parallel to the crystalline c axis [Fig. 1(c)]. The conduction band is formed by the highest occupied molecular orbital (HOMO) on the Pc ring, while the localized next HOMOs are mainly constructed by the Fe $3d$ orbitals. Here, the electronic structure on Fe^{3+} takes a low-spin state ($S = 1/2$) in the axial crystal field. Due to the appropriate amount of on-site and nearest-neighbor Coulomb interactions, this electronic structure stabilizes the charge disproportionation with decreasing temperature [19,20]. On the other hand, the antiferromagnetic (AFM) order of the local magnetic moment on Fe sites also develops via the intermolecular interaction J_{dd} [21]. Depending on the sign of $J_{\pi d}$, which has been controversial for some time and still remains to be settled [22–26], it is thought that two types of ground states are realized as shown in Figs. 1(d) and 1(e). In both cases, whether $J_{\pi d}$ works for FM or AFM, it can prevent the charge transfer to the neighboring site and thus assist in the enhancement of the effective Coulomb interactions to localize the charge carrier. Therefore, once the AFM order on Fe sites is broken by a magnetic field, the charge carrier drastically obtains itinerancy [Fig. 1(f)]. This is the origin of the giant magnetoresistance in $TPP[Fe(Pc)(CN)_2]_2$. Note that the isostructural $TPP[Co(Pc)(CN)_2]_2$ without local magnetic moment ($J_{\pi d} = 0$) does not exhibit negative magnetoresistance. Thus, $J_{\pi d}$ is an important parameter dominating the molecular conductivity and in this regard, it corresponds to the Hund coupling between itinerant e_g- and localized t_{2g}-electron spins in the perovslite manganites with giant magnetoresistance [27]. Therefore, experimental clarification of the basic properties of $J_{\pi d}$ in $Fe(Pc)(CN)_2$, i.e., whether it works as FM or AFM and its magnitude, is highly desired.

One simple strategy for the precise evaluation of $J_{\pi d}$ is just to expand the intermolecular distance so as to neglect J_{dd} with the Pc structure intact and then measure its magnetization. Without J_{dd}, the net magnetic moment on a single Pc element, i.e., the π-electron spin and $3d$ moment combined by $J_{\pi d}$, should behave like a free spin and follow Curie's law. In this case, we can explicitly evaluate the nature of $J_{\pi d}$ (FM or AFM) from the Curie constant C. Furthermore, we have a chance to determine its magnitude once we can detect a nonlinear change of Curie constant which should happen in the temperature region around $J_{\pi d}/k_B$. Thus, magnetization measurement of the isolated molecular solvent is a powerful technique to investigate the $J_{\pi d}$ nature especially when magnitude of $J_{\pi d}$ is comparable with J_{dd}. If we can make sure that $J_{\pi d}$ is much larger than J_{dd} by the above method, magnetization measurement of the crystalline π radical $Fe(Pc)(CN)_2$ is also applicable to determine its $J_{\pi d}$ magnitude.

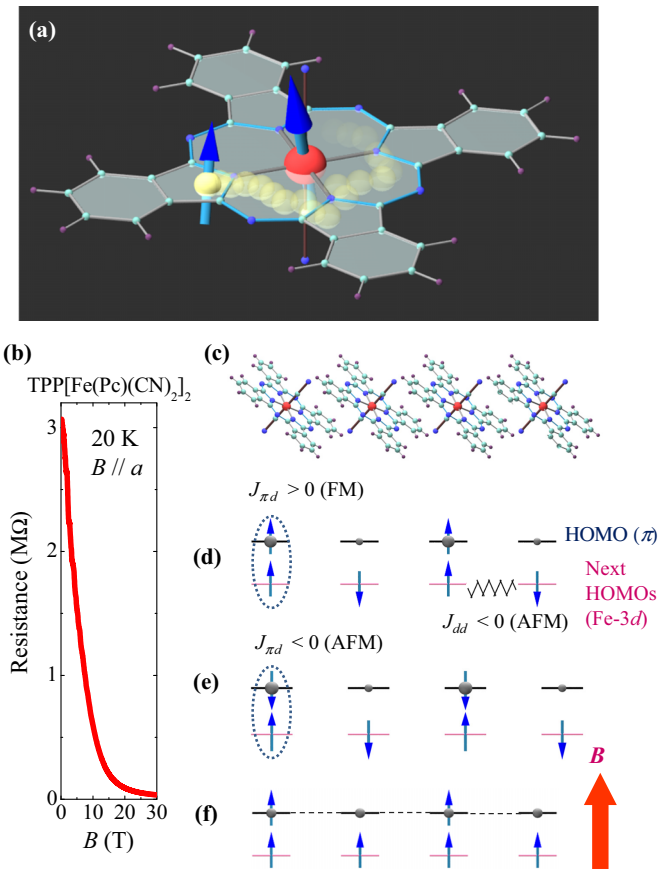

FIG. 1. (Color online) (a) Schematic image of the intramolecular magnetic interaction (π-d interaction) in the phthalocyanine (Pc) molecule. Here, the arrow and central (itinerant) sphere denote the spin and transition metal ion (π electron), respectively. (b) Giant magnetoresistance in TPP[Fe(Pc)(CN)$_2$]$_2$ quoted from Ref. [17]. (c) The one-dimensional stacking structure of the Pc ring in TPP[Fe(Pc)(CN)$_2$]$_2$. (d) and (e) Possible ground states realized by an FM (d) and AFM (e) π-d interaction in TPP[Fe(Pc)(CN)$_2$]$_2$. The diameter of the sphere reflects the existence probability in the charge disproportionation state stabilized by effective on-site and nearest-neighbor Coulomb interactions. (f) Magnetic-field-induced conducting state, where the AFM order of the localized Fe moment is broken.

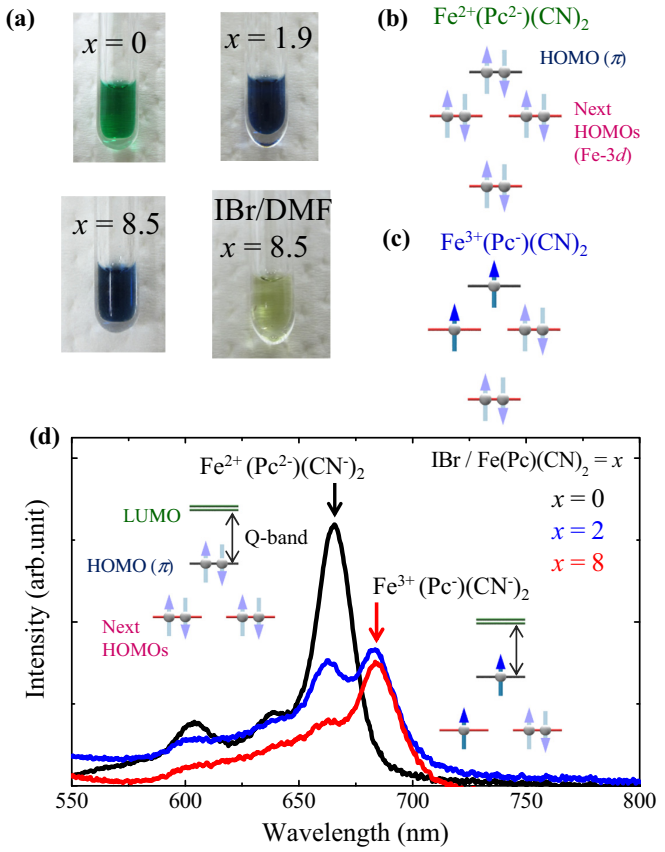

FIG. 2. (Color online) (a) Fe(Pc)(CN)$_2$/DMF solvent with various IBr concentrations x. The light yellow one is the IBr/DMF solvent without Fe(Pc)(CN)$_2$. (b) and (c) Electronic structure of (b) $Fe^{2+}(Pc^{2-})(CN^-)_2$ and (c) oxidized $Fe^{3+}(Pc^-)(CN^-)_2$. (d) Absorption spectra of the Fe(Pc)(CN)$_2$ + xIBr/DMF solvent with x = 0,2, and 8 at room temperature.

II. EXPERIMENT

For this purpose, first we attempted to obtain a single molecular solvent by using $K_2^+[Fe^{2+}(Pc^{2-})(CN^-)_2]$ powder in dimethylformamide (DMF). Here, K_2[Fe(Pc)(CN)$_2$] powder crystal is obtained from commercially available Fe(Pc) and KCN by refluxing in ethanol and is purified by recrystallization as precipitates in acetone. In Fig. 2(a), the picture of $x = 0$ shows the solution of Fe(Pc)(CN)$_2$/DMF solvents of $\approx 5 \times 10^{-4}$ mol/L concentration. Note that at this stage, dissolved $Fe^{2+}(Pc^{2-})(CN^-)_2$ has a closed shell and thus, is nonmagnetic [Fig. 2(b)] [28]. Next, we move on to generate spins both in HOMO (π orbital on the Pc ring) and next HOMOs (localized 3d-like orbitals) in Fe(Pc)(CN)$_2$ through oxidization. As a strong oxidant, we have used iodine bromide (IBr) and prepared its DMF solvent. Through the addition of IBr/DMF into $K_2^+[Fe^{2+}(Pc^{2-})(CN^-)_2]$/DMF, the following chemical reaction is expected to occur:

$$K^+_2[Fe^{2+}(Pc^{2-})(CN^-)_2] + 4IBr \rightleftarrows Fe^{3+}(Pc^-)(CN^-)_2 + 2(K^+ + IBr_2^-) + I_2. \quad (1)$$

Here, both oxidized HOMO and the next HOMOs in $Fe^{3+}(Pc^-)(CN^-)_2$ have magnetic moment [Fig. 2(c)]. We prepared the Fe(Pc)(CN)$_2$ solvents with various IBr concentrations from x = 0–11 without precipitation. Here, x denotes the molar ratio of supplied IBr to Fe(Pc)(CN)$_2$ [x = IBr/Fe(Pc)(CN)$_2$]. As shown in Fig. 2(a), the solvent with $x = 0$ shows a green color originating from the divalent iron in Fe(Pc)(CN)$_2$. With the IBr titration, the solvent immediately turns bluish, indicating the generation of trivalent iron (Fe^{3+}) through the oxidization.

For the magnetization measurements, 40 μL solvent with various IBr concentrations x was dropped into the bottom of a plugged quartz tube with external and internal diameters of 5 and 3 mm, respectively. In order to exclude air, especially oxygen, the inner space is carefully pumped, keeping the solvent frozen at the bottom of the quartz tube immersed in the liquid nitrogen. After final pumping, the quartz tube is sealed with 7-cm length. Then, magnetization measurements have been performed by the DC SQUID magnetometer.

For the measurements in high temperature region, Fe^{3+} (Pc^{-}) $(CN^{-})_2 \cdot 2CHCl_3$ single crystals was fabricated by the electrochemical oxidation of $(THA^{+})[Fe^{3+}(Pc^{2-})\ (CN^{-})_2]$ in a mixed solvent of acetonitrile and chloroform, under a constant current of 0.5 μA. Here, THA denotes tetraheptylammonium. In advance, $(THA^{+})_2$ $[Fe^{2+}(Pc^{2-})\ (CN^{-})_2]$ is obtained from K_2 $[Fe(Pc)(CN)_2]$ through the cation exchange carried out by metathesis using tetraheptylammonium iodide. Then it was oxidized to $(THA^{+})[Fe^{3+}(Pc^{2-})\ (CN^{-})_2]$ by bromine. Crystal structure of the obtained $Fe(Pc)(CN)_2 \cdot 2CHCl_3$ was identified by the x-ray diffraction method.

III. RESULTS AND DISCUSSIONS

In order to obtain microscopical information, we performed the optical measurements in the visible region at room temperature. We focus on the so-called Q-band peak, which is a characteristic absorption that corresponds to the energy gap between HOMO and double degenerate lowest unoccupied molecular orbital (LUMO) in a Pc ring [15,29–31] [see Fig. 2(d)]. As shown in Fig. 2(d), observation of the sharp Q-band peak at $\lambda \approx 665$ nm guarantees that the Pc ring is preserved in the DMF solvent. At $x = 2$, an additional new peak structure appears in a slightly longer wave region at $\lambda = 685$ nm, indicating the Q band of an oxidized trivalent $Fe^{3+}(Pc)(CN)_2$ [30]. As x increases, the intensity balance between the original and new Q-band peak is changed and only the new peak can be seen at $x = 8$, implying the full oxidization of the Fe site ($Fe^{2+} \rightarrow Fe^{3+}$). Furthermore, the near-half-intensity Q-band peak at $x = 8$ compared with that at $x = 0$ indicates the full oxidization of the Pc ring ($Pc^{2-} \rightarrow Pc^{-}$), because its intensity depends on the number of π electrons in HOMO.

Figure 3(a) shows the magnetization of the oxidized $Fe(Pc)(CN)_2$ solvent ($x = 6.3$) and its background (B.G.) contribution $\chi_{B.G.}$, mainly comes from the temperature-independent core diamagnetism of DMF, IBr, and the surrounding quartz tube. The much smaller paramagnetic contribution in $\chi_{B.G.}$ relative to the net magnetization of $Fe(Pc)(CN)_2$ ensures the experimental accuracy for the C evaluation. Figure 3(b) shows the net magnetic susceptibility of $Fe(Pc)(CN)_2$ ($\Delta\chi$) with various x after subtraction of the B.G. paramagnetic and diamagnetic contributions. As mentioned later, the temperature-independent diamagnetic term A can be derived as a slope of the linear fitting line [inset in Fig. 3(c)]. With increasing x, a monotonic increase of $\Delta\chi$ is observed up to $x = 8.5$, indicating generation of the unpaired spin through the oxidization [32]. The π-d character (FM or AFM) can be identified as the Curie constant which reflects a magnitude of an effective magnetic moment. Under the present magnetic field of 10 kOe, magnetic susceptibility follows the simple relation of $\chi = C/T + A$ above 10 K. Therefore, assuming that $J_{\pi d}$ is larger than the energy scale of the measuring temperature, Curie constant can be deduced as the intercept of the extrapolation of the linear fitting line of χT [see inset in Fig. 3(c)]. Here, fitting range is fixed between 10 and 50 K for all samples ($x = 0 \sim 11$). The clear linearity of χT in this temperature region guarantees that $J_{\pi d}$ in a FePc ring is sufficiently larger than 50 K. This is consistent with the fact that the negative magnetoresistance originating from the

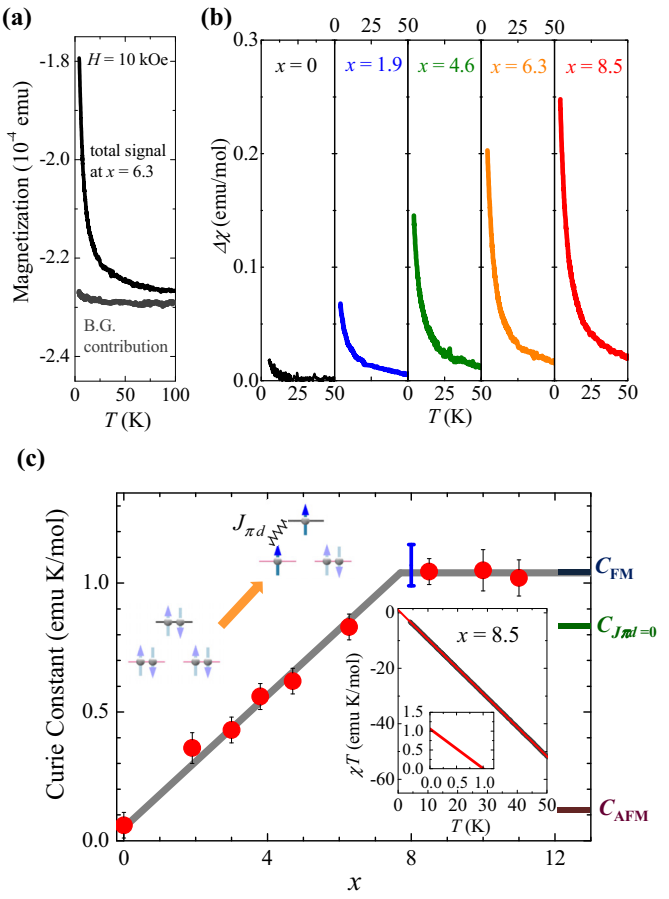

FIG. 3. (Color online) (a) Typical example of the magnetization of the $Fe(Pc)(CN)_2 + 6.3$ IBr/DMF and its background contribution (IBr/DMF). (b) Temperature dependence of the net magnetic susceptibility of $Fe(Pc)(CN)_2$ with various values of x after subtraction of the background (B.G.) terms. (c) Curie constant determined as the intercept of the extrapolation of the linear fitting line of χT (including diamagnetic term) as shown in the inset. The constants obtained with Br_2 oxidant at $x = 8$ are within the longitudinal blue bar. The theoretical values of C in the cases of the FM ($J_{\pi d}/k_B > 100$ K), PM ($J_{\pi d}/k_B = 0$ K), and AFM ($J_{\pi d}/k_B < -100$ K) π-d interactions are marked as horizontal bars on the right ordinate.

π-d interaction can be seen up to 70 K [17]. Figure 3(c) shows the obtained Curie constant as a function of x. The saturation value of $C = 1.04$ emuK/mol is significantly larger than the case with $J_{\pi d} = 0$ ($C = 0.83$ emuK/mol) and is realized when a ferromagnetically coupled magnetic moment ($m = m^d + m^e = 3\mu_B$) is locked in a position perpendicular to the Pc plane [see the schematic in Fig. 4(a), as well as the Appendix]. Here, $m^d = 2\mu_B$ [33] and $m^e = \mu_B$ are the localized d- and itinerant π-electron's magnetic moments, respectively. In order to check the saturation of C, we have prepared a doubling dilution solvent at $x = 11$ and obtained a similar result ($C = 1.03 \pm 0.07$ emuK/mol). Furthermore, we also confirmed this by obtaining $C = 1.07 \pm 0.08$ emuK/mol when using the stronger oxidant Br_2 ($x = 8$) in the doubling dilution solvents as shown by the longitudinal blue bar in Fig. 3(c). Therefore, we conclude that the ferromagnetic π-d interaction exists in $Fe(Pc)(CN)_2$.

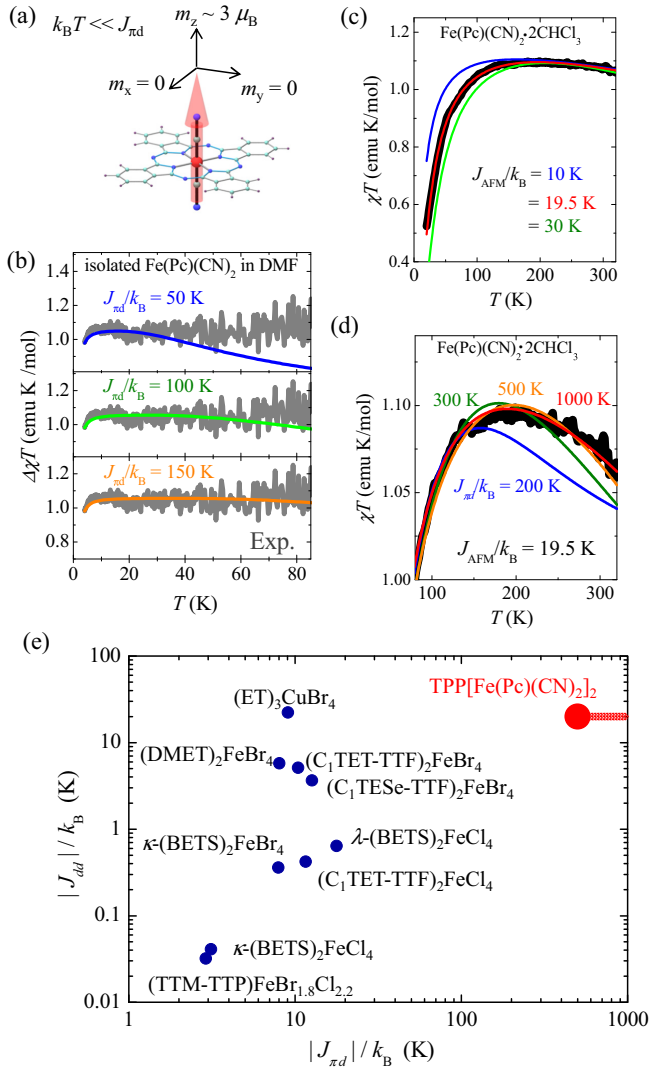

FIG. 4. (Color online) (a) Magnetic anisotropy in the $Fe^{3+}(Pc^-)$ $(CN)_2$ molecular unit. The arrow indicates the net magnetic moment pinned along the z direction. (b) Comparison of $\Delta\chi T$ between the experimental data ($x = 8.5$) and calculation curves with $J_{\pi d}/k_B = 50, 100$, and 150 K with arbitrary offsets. (c) Temperature dependence of χT of single crystals of the neutral π radical $Fe(Pc)(CN)_2 \cdot 2CHCl_3$ with random orientation, which is well reproduced by $1.34\exp(-J_{AFM}/k_BT) - 6 \times 10^{-4}T$ with $J_{AFM}/k_B = 19.5$ K (red line). (d) Comparison of χT between the experimental data in (c) and calculation curves with $J_{AFM}/k_B = 19.5$ K, $J_{\pi d}/k_B = 200, 300, 500$, and 1000 K. (e) Relations between $|J_{dd}|$ and $|J_{\pi d}|$ in representative π-d systems [8].

Finally, we evaluated the magnitude of the ferromagnetic $J_{\pi d}$. We tried to detect a deviation from the linearity in $\Delta\chi T$, which should happen in the temperature region around $J_{\pi d}/k_B$. Figure 4(b) shows the $\Delta\chi T$ of the $x = 8.5$ sample up to 85 K as well as the theoretical calculations with $J_{\pi d}/k_B = 50, 100$, and 150 K. The infinitesimal amount of the sample ($\sim 2 \times 10^{-8}$ mol) in the solvent limits the temperature region for the precise evaluation below 100 K. In this case, remarkable deviation from the linearity could not be detected within the experimental accuracy, indicating that $J_{\pi d}$ is larger than 100 K. This is consistent with the previous results of the scanning tunneling microscopy measurements (21 meV) and density functional theory (36 meV) for CuPc adsorbed on the Ag(100) surface [34]. In order to increase the resolution to detect the $J_{\pi d}$ contribution in the higher temperature region, we have measured magnetization of the single crystals of the neutral π radical $Fe^{3+}(Pc^-)$ $(CN^-)_2 \cdot 2CHCl_3$ [35] ($\sim 6 \times 10^{-6}$ mol) up to 320 K, assuming that $J_{\pi d}$ is much larger than the intermolecular antiferromagnetic interaction $J_{AFM} = |J_{dd}|$. Figure 4(c) shows the temperature dependence of χT of $Fe(Pc)(CN)_2 \cdot 2CHCl_3$ single crystals with random orientation. Based on the result that the ferromagnetic $J_{\pi d}/k_B$ is larger than 100 K, J_{AFM} is unambiguously determined as a fitting parameter to reproduce the continuous decrease of χT in the low temperature region [see the comparison with calculation lines with various values of J_{AFM}/k_B in Fig. 4(c)]. In the present case, it is noteworthy that the experimental χT is well reproduced only by the simple formula of $A\exp(-J_{AFM}/k_BT) + aT$ with $J_{AFM}/k_B = 19.5$ K, $A = 1.34$, and $a = -6 \times 10^{-4}$ up to 320 K, indicating that $J_{\pi d}$ is large enough to saturate the total magnetic moment in this temperature region. The slight deviation of A from 1.04 comes from the insufficiency of the random orientation in finite numbers of crystals and the tiny value of a may come from the temperature-independent diamagnetic background. Comparisons between experimental χT and theoretical calculations including antiferromagnetic intermolecular interaction $J_{AFM}/k_B = 19.5$ K and ferromagnetic intramolecular interaction $J_{\pi d}/k_B = 200 \sim 1000$ K are shown in Fig. 4(d). For the strict evaluation, finite ambiguity of the temperature linear term and the amplitude A in each calculation are determined to minimize the deviation from the experimental curvature. As a result, we can see that $J_{\pi d}/k_B > 500$ K is required to reproduce the experimental data. This magnitude is more than one-order larger than those among the known π-d systems [8] [see Fig. 4(e)].

According to the theoretical model by Matsuura *et al.* [26], the π-d coupling in $Fe(Pc)(CN)_2$ is not originating from the superexchange interaction between d and HOMO [36] because there is no hybridization between them. Instead, it is caused by the Hund-like ferromagnetic coupling between HOMO and the other molecular orbitals, in which unpaired spin is virtually induced through the superexchange process with the d orbital. Among several superexchange paths in Ref. [26], those between d- and doubly degenerate molecular orbitals just below HOMO are considered to be dominant for the observed large ferromagnetic π-d coupling. Thus, the molecular structure surrounding the magnetic ion with tetragonal symmetry has a great advantage for huge π-d coupling in terms of the larger hybridization and doubling the dominant superexchange path between d and molecular orbitals.

IV. CONCLUSIONS

In summary, we have revealed that giant ferromagnetic intramolecular interaction (>500 K) exists in the $Fe(Pc)(CN)_2$ molecule through the magnetization measurements of its isolated solution and the single crystals of its neutral π radical $Fe(Pc)(CN)_2 \cdot 2CHCl_3$. The Curie constant of the sufficiently oxidized $Fe(Pc)(CN)_2$ single molecule with an unpaired π-electron spin and a localized d-electron's magnetic moment

is quantitatively explained by assuming the ferromagnetic coupling between them. The molecular compound with such a large ferromagnetic π-d interaction is of great advantage for realizing the molecular ferromagnet via the double exchange mechanism, by optimization of the intermolecular overlap.

ACKNOWLEDGMENTS

The authors thank H. Tajima and T. Inabe for fruitful discussion. This work was in part supported by a Grant-In-Aid for Scientific Research from Japan Society for the Promotion of Science (Grants No. 24340084 and No. 25800196), and Yamada Science Foundation.

APPENDIX: CALCULATION OF THE MAGNETIC SUSCEPTIBILITY

Based on the empirical result that the large magnetic anisotropy in a phthalocyanine (Pc) molecule is still observed even at room temperature [33], we suppose that the localized magnetic moment on the Fe site ($2\mu_B$) is locked to be parallel to the z direction (perpendicular to the Pc plane) [see Fig. 4(a)]. In this case, orientation of the π-electron spin (μ_B) in isolated $Fe(Pc)(CN)_2$ is determined by the balance between the external magnetic field and the effective field ($J_{\pi d}/\mu_B$) along the z direction. According to the statistical mechanics, magnetic susceptibility along the z direction is calculated from the following equation:

$$\chi_z = \frac{N}{H}\frac{\left[3\mu_B \exp\left(\frac{J_{\pi d}}{k_B T}\right)\sinh\left(\frac{3\mu_B H}{k_B T}\right)+\mu_B \exp\left(\frac{-J_{\pi d}}{k_B T}\right)\sinh\left(\frac{\mu_B H}{k_B T}\right)\right]}{\left[\exp\left(\frac{J_{\pi d}}{k_B T}\right)\cosh\left(\frac{3\mu_B H}{k_B T}\right)+\exp\left(-\frac{J_{\pi d}}{k_B T}\right)\cosh\left(\frac{\mu_B H}{k_B T}\right)\right]}. \tag{A1}$$

On the other hand, magnetic susceptibility along the magnetic hard axis (x and y directions) is deduced as follows. When the external field is applied along the x direction, Hamiltonian for the π electron spin can be expressed as

$$\mathcal{H} = \begin{pmatrix} J_{\pi d} & \mu_B H_x \\ \mu_B H_x & -J_{\pi d} \end{pmatrix}. \tag{A2}$$

The eigenvector of the ground state with $E = -\sqrt{J_{\pi d}^2 + (\mu_B H_x)^2}$ is

$$\boldsymbol{a} \approx \frac{1}{\sqrt{4J_{\pi d}^2 + (\mu_B H_x)^2}}\begin{pmatrix} 2J_{\pi d} \\ \mu_B H_x \end{pmatrix}. \tag{A3}$$

Therefore,

$$\chi_x \propto \boldsymbol{a}^\dagger \begin{pmatrix} 0 & 1 \\ 1 & 0 \end{pmatrix}\boldsymbol{a} = \frac{4J_{\pi d}\mu_B H_x}{4J_{\pi d}^2 + (\mu_B H_x)^2} \sim \left(\frac{\mu_B H_x}{J_{\pi d}}\right). \tag{A4}$$

In the present case with $H_x = 10\,\mathrm{kOe}$ ($\mu_B H_x/k_B \sim 0.67\,\mathrm{K}$) and $J_{\pi d}/k_B > 100\,\mathrm{K}$, the contribution of χ_x and χ_y with $g^e = 2$ is negligible because

$$\chi_x \sim \left(\frac{M^e}{M^{\mathrm{total}}}\right)^2 \times \frac{\mu_B H_x}{J_{\pi d}}\chi_z \sim 10^{-3}\chi_z. \tag{A5}$$

In the solution, the Pc ring is randomly oriented and therefore, the z component of magnetic susceptibility for each Pc ring should be $\chi_z \cos\theta$, where θ is the angle between the z direction of a Pc ring and an external magnetic field direction. Thus, the net magnetic susceptibility χ is given as the average of the projection component of $\chi_z \cos\theta$ onto the magnetic-field direction ($\chi_z \cos^2\theta$) and expressed as

$$\chi = \frac{\chi_z}{4\pi}\int_0^{2\pi} d\phi \int_0^{\pi} \cos^2\theta \sin\theta d\theta = \frac{1}{3}\chi_z. \tag{A6}$$

In the case of single crystals of $Fe(Pc)(CN)_2 \cdot 2CHCl_3$, magnetic susceptibility with intermolecular interaction is calculated from multiplication of Eq. (A1) by a factor of $\exp(-\frac{J_{\mathrm{AFM}}}{k_B T})$.

[1] H. Kobayashi, H. Tomita, T. Naito, A. Kobayashi, F. Sakai, T. Watanabe, and P. Cassoux, J. Am. Chem. Soc. **118**, 368 (1996).
[2] L. Brossard, R. Clerac, C. Coulon, M. Tokumoto, T. Ziman, D. K. Petrov, V. N. Laukhin, M. J. Naughton, A. Audouard, F. Goze, A. Kobayashi, H. Kobayashi, and P. Cassoux, Eur. Phys. J. B **1**, 439 (1998).
[3] E. Ojima, H. Fujiwara, K. Kato, and H. Kobayashi, J. Am. Chem. Soc. **121**, 5581 (1999).
[4] H. Akutsu, K. Kato, E. Ojima, H. Kobayashi, H. Tanaka, A. Kobayashi, and P. Cassoux, Phys. Rev. B **58**, 9294 (1998).
[5] Y. Kashimura, H. Sawa, S. Aonuma, R. Kato, H. Takahashi, and N. Mori, Solid State Commun. **93**, 675 (1995).
[6] S. Uji, H. Shinagawa, T. Terashima, T. Yakabe, Y. Terai, M. Tokumoto, A. Kobayashi, H. Tanaka, and H. Kobayashi, Nature (London) **410**, 908 (2001).
[7] L. Balicas, J. S. Brooks, K. Storr, S. Uji, M. Tokumoto, H. Tanaka, H. Kobayashi, A. Kobayashi, V. Barzykin, and L. P. Gorkov, Phys. Rev. Lett. **87**, 067002 (2001).
[8] T. Mori and M. Katsuhara, J. Phys. Soc. Jpn. **71**, 826 (2002).
[9] N. Ishikawa, M. Sugita, T. Ishikawa, S. Koshihara, and Y. Kaizu, J. Am. Chem. Soc. **125**, 8694 (2003).
[10] N. Ishikawa, M. Sugita, T. Ishikawa, S. Koshihara, and Y. Kaizu, J. Phys. Chem. B **108**, 11265 (2004).
[11] M. Urdampilleta, S. Klyatskaya, J. P. Cleuziou, M. Ruben, and W. Wernsdorfer, Nat. Mater. **10**, 502 (2011).
[12] R. Vincert, S. Klyatskaya, M. Ruben, W. Wernsdorfer, and F. Balestro, Nature (London) **488**, 357 (2012).
[13] S. Thiele, F. Balestro, R. Ballou, S. Klyatskaya, M. Ruben, and W. Wernsdorfer, Science **344**, 1135 (2014).
[14] T. Inabe and H. Tajima, Chem. Rev. **104**, 5503 (2004).

[15] M. Matsuda, T. Naito, T. Inaba, N. Hanasaki, H. Tajima, T. Otsuka, K. Agawa, B. Narymbetov, and H. Kobayashi, J. Mater. Chem. **10**, 631 (2000).
[16] N. Hanasaki, H. Tajima, M. Matsuda, T. Naito, and T. Inabe, Phys. Rev. B **62**, 5839 (2000).
[17] N. Hanasaki, M. Matsuda, H. Tajima, E. Ohmichi, T. Osada, T. Naito, and T. Inaba, J. Phys. Soc. Jpn. **75**, 033703 (2006).
[18] M. Kimata, Y. Takahide, A. Harada, H. Satsukawa, K. Hazama, T. Terashima, S. Uji, T. Naito, and T. Inabe, Phys. Rev. B **80**, 085110 (2009).
[19] N. Hanasaki, K. Masuda, K. Kodama, M. Matsuda, H. Tajima, J. Yamazaki, M. Takigawa, J. Yamamura, E. Ohmichi, T. Osada, T. Naito, and T. Inaba, J. Phys. Soc. Jpn. **75**, 104713 (2006).
[20] H. Seo and H. Fukuyama, J. Phys. Soc. Jpn. **66**, 1249 (1997).
[21] H. Tajima, G. Yoshida, M. Matsuda, K. Nara, K. Kajita, Y. Nishio, N. Hanasaki, T. Naito, and T. Inabe, Phys. Rev. B **78**, 064424 (2008).
[22] D. E. C. Yu, M. Matsuda, H. Tajima, A. Kikuchi, T. Taketsugu, N. Hanasaki, T. Naito, and T. Inabe, J. Mater. Chem. **19**, 718 (2009).
[23] Y. Otsuka, H. Seo, and Y. Motome, Physica B **405**, S317 (2010).
[24] C. Hotta, M. Ogata, and H. Fukuyama, Phys. Rev. Lett. **95**, 216402 (2005).
[25] C. Hotta, Phys. Rev. B **81**, 245104 (2010).
[26] H. Matsuura, M. Ogata, K. Miyaka, and H. Fukuyama, J. Phys. Soc. Jpn. **81**, 104705 (2012).
[27] A. Urushibara, Y. Moritomo, T. Arima, A. Asamitsu, G. Kido, and Y. Tokura, Phys. Rev. B **51**, 14103 (1995).
[28] In reality, the tiny amount of $K^+[Fe^{3+}(Pc^{2-})\ (CN^-)_2]$ $(S = 1/2)$ is mixed, which can be detected as a finite magnetization at $x = 0$ in Fig. 3(b).
[29] E. A. Ough and M. J. Stillman, Inorg. Chem. **33**, 573 (1994).
[30] E. A. Ough and M. J. Stillman, Inorg. Chem. **34**, 4317 (1995).
[31] D. R. Tackley, D. Geoffrey, and S. M. Ewen, Phys. Chem. Chem. Phys. **3**, 1419 (2001).
[32] In Eq. (1), oxidization and reduction reactions are balanced depending on the IBr amount. In the present case in the DMF solvent, an excess amount of IBr ($x = 8$) is required to achieve full oxidization of $K_2^+[Fe^{2+}(Pc^{2-})\ (CN^-)_2]$ to $Fe^{3+}(Pc^-)\ (CN^-)_2$.
[33] N. Hanasaki, M. Matsuda, H. Tajima, T. Naito, and T. Inabe, J. Phys. Soc. Jpn. **72**, 3226 (2003).
[34] A. Mugarza, C. Krull, R. Robles, S. Stepanow, G. Ceballos, and P. Gambardella, Nat. Commun. **2**, 490 (2011).
[35] K. Morimoto and T. Inabe, J. Mater. Chem. **5**, 1749 (1995).
[36] In Ref. [26], they define "HOMO" as a highest occupied molecular orbital for "charge neutral Pc." Therefore, "LUMO" in their definition corresponds to "HOMO" in our definition for negatively charged Pc in $Fe^{3+}(Pc^-)\ (CN^-)_2$ or $Fe^{2+}(Pc^{2-})\ (CN^-)_2$.